Monitoring of Selected Skin-Borne Volatile Markers of Entrapped Humans by Selective Reagent Ionization Time of Flight Mass Spectrometry in NO⁺ Mode

Paweł Mochalski,*,[†] Karl Unterkofler,[‡] Hartmann Hinterhuber,[§] and Anton Amann*,[†,∥]

[†]Breath Research Institute, University of Innsbruck, Rathausplatz 4, A-6850 Dornbirn, Austria
[‡]Vorarlberg University of Applied Sciences, Hochschulstrasse 1, A-6850 Dornbirn, Austria
[§]Univ.-Clinic for Psychiatry, Innsbruck Medical University, Anichstr, 35, A-6020 Innsbruck, Austria
[∥]Univ.-Clinic for Anesthesia and General Intensive Care, Innsbruck Medical University, Anichstr, 35, A-6020 Innsbruck, Austria

ABSTRACT: Selective reagent ionization time-of-flight mass spectrometry with NO⁺ as the reagent ion (SRI-TOF-MS (NO⁺)) was applied for near real-time monitoring of selected skin-borne constituents which are potential markers of human presence. The experimental protocol involved a group of 10 healthy volunteers enclosed in a body plethysmography chamber mimicking the entrapment environment. A total of 12 preselected omnipresent in human scent volatiles were quantitatively monitored. Among them there were six aldehydes (n-propanal, n-hexanal, n-heptanal, n-octanal, n-nonanal, and 2 methyl 2-propenal), four ketones (acetone, 2-butanone, 3-buten-2-one, and 6-methyl-5-hepten-2-one), one hydrocarbon (2-methyl 2-pentene), and one terpene (DL-limonene). The observed median emission rates ranged from 0.28 to 44.8 nmol × person⁻¹ × min⁻¹ (16−1530 fmol × cm⁻² × min⁻¹). Within the compounds under study, ketones in general and acetone in particular exhibited the highest abundances. The findings of this study provide invaluable information about formation and evolution of a human-specific chemical fingerprint, which could be used for the early location of entrapped victims during urban search and rescue operations (USaR).
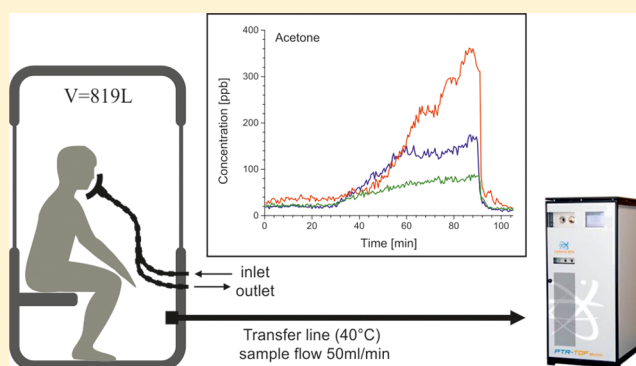
Hundreds of volatile organic compounds (VOCs) are emitted through breath, urine, and skin emanations by a human body.[1,2] This specific chemical fingerprint mirrors human physiology and can be used as a noninvasive biochemical probe capable of tracing normal and disease processes occurring in the organism, environmental exposure to pollutants and/or toxins, or microorganisms' activity.[3] Recently, an effort was made to employ this chemical signature for safety and security applications. There is growing evidence provided by a number of recent studies suggesting that the chemical analysis of human scent could considerably improve the effectiveness of search and rescue operations (USaR) organized after disasters entailing building collapses (e.g., earthquakes, tropical storms, explosions).[4] Although USaR teams increasingly rely on specialized technical equipment supporting the rapid detection of trapped humans, trained rescue dogs are still their preferred choice.[5] Canines search rapidly and effectively disaster areas; however, they are stress-prone and exhibit limited active time.[6] Bearing in mind the recent high sequence of natural or man-made disasters it is reasonable to assume that the demand for novel human detectors will markedly increase in the nearest future.[7]

In our recent study, we identified and quantified 33 volatile organic compounds omnipresent in forearm skin emanations of healthy volunteers.[8] However, the main goal of that study was the reliable identification and detection of skin-borne species. To meet the strict demands, forearm skin was used during experiments. Forearm skin exhibits some differences as compared to the other parts of the body that is reflected by the lower concentration of the sebaceous glands and different composition of their secretion.[9] Consequently, the emission rates of some volatiles presented in our recent paper could differ from the ones typical for other parts of the body. The main goal of the present study was the real-time monitoring of the whole-skin emission of the selected potential markers of human presence in conditions mimicking entrapment.

Proton-transfer reaction mass spectrometry[10] is a well-established powerful tool in the analyst arsenal for detection and quantification of volatile organic compounds in biological, medical, and environmental studies.[11−13] This position stems from its versatility, excellent sensitivity (low ppt concentration levels), and real-time response. Recent employing of a time-of-flight (TOF) mass filter in the proton transfer reaction-mass spectrometry (PTR-MS) instruments considerably increased

their resolving power (up to 5000 $m/\Delta m$) and, thereby, the separation and identification of isobaric compounds.[14,15] Moreover, the analytical power of the PTR-TOF-MS can be further enhanced by employing different precursor ions instead of H_3O^+ such as NO^+, O_2^+, or Kr^+ (selective reagent ionization time-of-flight mass spectrometry (SRI-TOF-MS)).[15,16] Such an approach can help in many cases to separate functional isomers. Within the present study, volatiles were quantified using the SRI-TOF-MS in conjunction with NO^+ as the reagent ion. The selection of this reactant ion arose from two reasons. First, it provided the separation of aldehydes from ketones (classes of compounds very well represented in skin emanations).[8,17] Second, molecular ions of aldehydes produced in NO^+ reactions fragment considerably less than the ones produced when these species are exposed to H_3O^+.

EXPERIMENTAL SECTION

Materials and Calibration Mixtures. Single-compound calibration mixtures were prepared from pure liquid substances. The reference substances with purities ranging from 95 to 99.8% were purchased from Sigma-Aldrich (Austria) and Fluka (Switzerland).

The preparation of gaseous calibration mixtures was described in detail in our recent article.[18] In brief, gaseous mixtures of less volatile species were produced by means of a GasLab calibration mixtures generator (Breitfuss Messtechnik, Germany). The generator provides gas mixtures containing solutes at the concentration range of low-ppb to 100 ppm at predefined humidity levels produced from pure liquid substances and purified air. However, in this study, pure substances were additionally diluted at ratios of 1:2000−1:3000 to reduce the resulting concentration levels. Effectively, gaseous standards exhibiting four levels absolute humidity (1−3.53%) with analytes volume fractions ranging from approximately 0.5 to 230 ppb were used during calibration and validation. Gaseous standards of highly volatile compounds (e.g., 2-methyl-2-pentene) were prepared by injecting and evaporating a few microliters of liquid analyte into evacuated 1-L glass bulbs (Supelco, Canada). The desired calibration levels were achieved by transferring appropriate volumes of the bulb standard into Tedlar bags (SKC Inc.) filled with predefined amounts of humidified zero air, the latter being produced by the GasLab generator. Calibration curves were obtained on the basis of six distinct concentration levels.

Human Subjects. A cohort of 10 healthy volunteers (7 males, 3 females, age range 23−56 years, median 30.5 years) was involved in the study. All subjects gave written informed consent to participate and completed a questionnaire describing their health, smoking status, as well as the recent food intake. The sample collection was approved by the Ethics Commission of Innsbruck Medical University. The volunteers were asked to be in a fasting condition for 12 h before the experiment to mimic the entrapment conditions. Apart from this no special dietary regimes were applied. Volunteers were also asked to refrain from the use of cosmetics, which could interfere with the human scent and lead to the saturation of the detector.

Body Chamber and Experiment Protocol. A body-plethysmography chamber BodyScope (Ganshorn Medicin Electronic GmbH, Germany) mimicking the entrapment conditions was used during the experiments, as shown in Figure 1. The cuboidal chamber is made up of steel and glass and has internal dimensions of 82 cm × 63 cm × 161 cm (approximate volume 819 L). It was equipped with a four-
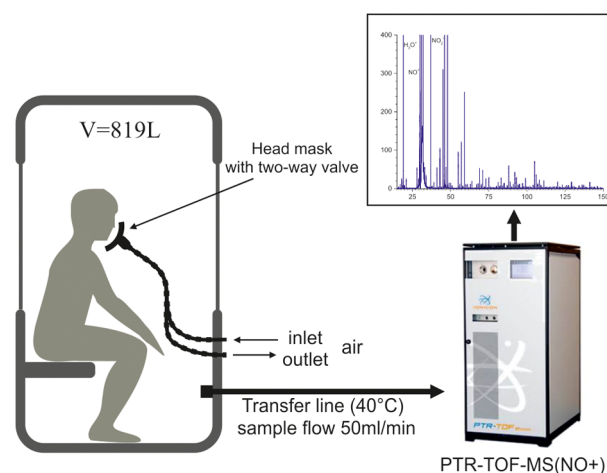

Figure 1. Experimental setup.

meter-long, heated (40 °C) Teflon transfer line (tube i.d. = 3.188 mm (1/8 in.)) connecting the chamber with the SRI-TOF-MS instrument. Since the highest level of the relative humidity of the chamber air observed during experiments was 90% for 27.5 °C, the transfer line temperature turned out to be sufficient to prevent water condensation and thereby loses of well soluble VOCs during sampling. The inlet of this sampling line was located in the center of the side wall, and the volatiles of interest were sampled at a steady flow rate of 50 ± 1 mL/min. It should be mentioned here that only a part of this stream (approximately 10 mL/min) was introduced into the drift tube of the SRI-TOF-MS instrument. When locked the chamber was gastight; however, its interior was connected with the outside air via an additional tube. Its task was to compensate the chamber pressure during sampling and to prevent the air exchange with the room air during the volunteer's spontaneous breathing. At the onset of an experiment, the chamber was filled with room air; however, an effort was made to reduce the level of the indoor contaminants. This was done by venting the laboratory room with outdoor air for several hours. Moreover, both volunteers and laboratory staff were asked to leave the room during this period. Prior to each experiment involving a human subject, a background measurement was performed. For this purpose the empty chamber was locked and the chamber air was sampled for 30 min using the SRI-TOF-MS settings as described below. Subsequently, the door was opened, the volunteer entered the chamber, and the door was locked again. All volunteers remained inside the chamber for 1 h in the sitting position. The duration of 1 h was selected, since longer periods were considered as inconvenient by the majority of subjects. The volunteers were dressed in underwear to uncover as large area of the skin as possible. Since the study was focused on skin-borne constituents of human scent it was necessary to separate the skin emanation from breath. This was done by a silicone head mask covering mouth and nose (V2Mask, Hans Rudolph Inc.) connected to a two-way nonrebreathing Y shape-valve (Hans Rudolph Inc.). The inlet and outlet of this valve were connected with flexible 22 mm tubes (Flextube, Intersurgical Inc., U.K.) to the additional ports located on the side wall of the chamber. Consequently, test subjects could freely inhale and exhale the outside air without contaminating the chamber air. After the volunteer had left the chamber, the door remained open and the monitoring of VOCs was continued for an additional 15 min. In total, a single experiment

Table 1. Reaction and Fragmentation Products of Species under Study in SRI-TOF-MS (NO$^+$)[a]

compound (purity)	formula	MW	reaction channel (dry air [%]/ wet air (RH = 3.5%) [%])	measured m/z [Th]	expected m/z [Th]	deviation [mTh]
n-propanal (98%)	C_3H_6O	58.08	$C_3H_6O + NO^+$ → $C_3H_5O^+$ + HNO (76%/100%)	57.0370	57.0335	3.5
			→ $C_2H_5^+$ + CO + HNO (18.6%/ 0%)	29.0386	29.0386	0.1
			→ $C_2H_3^+$ + CHO + H$_2$ + NO (5.5%/ 0%)	27.0266	27.0230	0.1
2-propenal, 2-methyl- (95%)	C_4H_6O	70.09	$C_4H_6O + NO^+$ → $C_4H_6O\cdot NO^+$ (1.5%/1.6%)	100.0488	100.0393	9.5
			→ $C_4H_5O^+$ + HNO (26%/22%)	69.0377	69.0335	4.2
			→ $C_3H_5^+$ + CO + HNO (73%/72%)	41.0419	41.0386	3.3
			→ $C_3H_3^+$ + CHO + NO + H$_2$ (10%/4.5%)	39.0264	39.0230	3.4
2-pentene, 2-methyl- (98%)	C_6H_{12}	84.16	$C_6H_{12} + NO^+$ → $C_6H_{12}^+$ + NO (39%/49.5%)	84.1004	84.0934	7.0
			→ $C_6H_{11}^+$ + HNO (0.8%/1%)	83.0933	83.0856	7.6
			→ $C_5H_9^+$ + CH$_3$NO (38.5%/35.5%)	69.0757	69.0699	5.8
			→ $C_4H_8^+$ + C$_2$H$_4$ + NO (2.8%/3%)	56.0660	56.0621	3.9
			→ $C_3H_5^+$ + C$_3$H$_7$NO (16.4%/9%)	41.0411	41.0386	2.5
			→ $C_3H_3^+$ + C$_3$H$_7$NO + H$_2$ (2.2%/1.6%)	39.0255	39.0230	2.6
acetone (99.8%)	C_3H_6O	58.08	$C_3H_6O + NO^+$ → $C_3H_6O\cdot NO^+$ (64%/65%)	88.0458	88.0394	6.4
			→ $C_2H_3O^+$ + CH$_3$NO (36%/35%)	43.0202	43.0179	2.3
n-hexanal (98%)	$C_6H_{12}O$	100.16	$C_6H_{12}O + NO^+$ → $C_6H_{11}O^+$ + HNO (12.5%/13.4%)	99.0856	99.0805	6.2
			→ $C_6H_9^+$ + H$_2$O + HNO (0.5%/0.5%)	81.0770	81.0698	7.1
			→ $C_5H_{11}^+$ + CO + HNO (14.2%/15.9%)	71.0902	71.0856	4.6
			→ $C_3H_7^+$ + C$_3$H$_5$O + NO (44.5%/48%)	43.0563	43.0543	2.1
			→ $C_3H_5^+$ + C$_3$H$_5$O + NO + H$_2$ (26.5%/21.2%)	41.0407	41.0386	2.1
			→ $C_3H_3^+$ + C$_3$H$_5$NO$_2$ + 2H$_2$ (1.8%/ 1.1%)	39.0242	39.0230	1.2
3-buten-2-one (99%)	C_4H_6O	70.09	$C_4H_6O + NO^+$ → $C_4H_6O\cdot NO^+$ (100%)	100.0461	100.0393	6.7
2-butanone (99.5%)	C_4H_8O	72.11	$C_4H_8O + NO^+$ → $C_4H_8O\cdot NO^+$ (82%/83%)	102.0616	102.0550	6.5
			→ $C_4H_8O^+$ + NO (2.2/2.1%)	72.0618	72.0570	4.8
			→ $C_3H_5O^+$ + CH$_3$NO (4.5%/4.6%)	57.0365	57.03350	2.9
			→ $C_2H_3O^+$ + C$_2$H$_5$NO (11%/10%)	43.0214	43.01785	3.5
n-heptanal (95%)	$C_7H_{14}O$	114.18	$C_7H_{14}O + NO^+$ → $C_7H_{13}O^+$ + HNO (18.2%/20%)	113.1031	113.0961	7.0
			→ $C_7H_{11}^+$ + H$_2$O + HNO (2.3%/2.2%)	95.0924	95.0856	6.8
			→ $C_6H_{13}^+$ + CO + HNO (8.7%/9.6%)	85.1076	85.1012	6.4
			→ $C_4H_9^+$ + C$_3$H$_5$O + NO (5.2%/4.8%)	57.0730	57.0699	3.1
			→ $C_3H_7^+$ + C$_4$H$_7$O + NO (39%/43%)	43.0562	43.0543	1.9
			→ $C_3H_5^+$ + C$_4$H$_7$O + NO + H$_2$ (25%/19.6%)	41.0404	41.0386	1.8
			→ $C_3H_3^+$ + C$_4$H$_7$O + NO + 2H$_2$ (1.8% /0.93%)	39.0239	39.0230	0.9
5-hepten-2-one, 6-methyl- (98%)	$C_8H_{14}O$	126.19	$C_8H_{14}O + NO^+$ → $C_7H_{12}O\bullet NO^+$ + CH$_2$ (4.6%/4.8%)*	142.1099	142.0869	23
			→ $C_8H_{14}O^+$ + NO (10.7/11.2%)	126.1134	126.1010	9.4
			→ $C_8H_{13}O^+$ + HNO (0.7/0.95%)	125.1053	125.0961	9.2
			→ $C_7H_{13}O^+$ + CHNO (1/1%)	113.1034	113.0961	7.3
			→ $C_8H_{12}^+$ + H$_2$O + NO (51/47.3%)	108.1017	108.0934	8.2
			→ $C_7H_9^+$ + H$_2$O + CH$_3$NO (21.7/16.9%)	93.0775	93.0699	7.6
			→ $C_6H_{10}^+$ + H$_2$O + C$_2$H$_2$ + NO (8.8/8.7%)	82.0838	82.0777	6.0
			→ $C_4H_7O^+$ + C$_4$H$_7$ + NO (2.1/2.7%)	71.0549	71.0492	5.7
			→ $C_2H_3O^+$ + C$_6$H$_{11}$ + NO (2.5/6.5%)	43.0205	43.0179	2.7
n-octanal (99%)	$C_8H_{16}O$	128.22	$C_8H_{16}O + NO^+$ → $C_8H_{15}O^+$ + HNO (27%/29.5%)	127.1204	127.1174	3.0
			→ $C_8H_{13}^+$ + H$_2$O + HNO (5.3% /5.2%)	109.1086	109.1012	7.4
			→ $C_5H_7^+$ + C$_3$H$_5$O + NO + 2H$_2$ (1.5% /1.5%)	67.0586	67.0542	4.4
			→ $C_4H_9^+$ + C$_4$H$_7$O + NO (57%/57%)	57.0734	57.0699	3.5
			→ $C_3H_5^+$ + C$_5$H$_9$O + NO + H$_2$ (8.5% /7%)	41.0407	41.0386	2.1
DL-Limonene (99%)	$C_{10}H_{16}$	136.23	$C_{10}H_{16} + NO^+$ → $C_{10}H_{16}^+$ + NO (21.5%/27%)	136.1329	136.1247	8.2
			→ $C_9H_{13}^+$ + CH$_3$NO (6.5%/6.9%)	121.1095	121.1012	8.3
			→ $C_8H_{11}^+$ + C$_2$H$_5$ + NO (4.7%/3.8%)	107.0953	107.0856	7.9
			→ $C_7H_{11}^+$ + C$_3$H$_5$ + NO (2%/2%)	95.0895	95.0856	4.0
			→ $C_7H_{10}^+$ + C$_3$H$_6$ + NO (21%/18.5%)	94.0838	94.0777	6.0
			→ $C_7H_9^+$ + C$_3$H$_7$ + NO (15.5%/13.5%)	93.0758	93.0699	6.0
			→ $C_7H_8^+$ + C$_3$H$_8$ + NO (19.7%/19.6%)	92.0679	92.0621	5.8
			→ $C_6H_8^+$ + C$_4$H$_8$ + NO (3.9%/3.6%)	80.0666	80.0621	4.5
			→ $C_6H_7^+$ + C$_4$H$_9$ + NO (4.7%/2.7%)	79.0602	79.0543	6.0
n-Nonanal (95%)	$C_9H_{18}O$	142.24	$C_9H_{18}O + NO^+$ → $C_9H_{17}O^+$ + HNO (46.2%/47.3%)	141.1373	141.1274	9.9
			→ $C_9H_{15}^+$ + H$_2$O + HNO (7.8%/6.9%)	123.1257	123.1168	8.9
			→ $C_5H_{11}^+$ + C$_4$H$_7$O + NO (8.4%/ 8.2%)	71.0916	71.0856	6.0
			→ $C_4H_9^+$ + C$_5$H$_9$O + NO (18%/18.2%)	57.0748	57.0699	4.9
			→ $C_3H_7^+$ + C$_6$H$_{11}$O + NO (15.7%/13.7%)	43.0580	43.0543	3.8
			→ $C_3H_5^+$ + C$_6$H$_{11}$O + NO + H$_2$ (4.18%/5.8%)	41.0405	41.0386	1.9

Table 1. continued

Table 2. Quantifier Ions [Th], LODs [ppb], RSDs [%], Coefficients of Variation (R^2), and Linear Ranges [ppb] for Compounds under Study[a]

compound	CAS	quantifier ion [Th]	LOD [ppb]	RSD [%]	R^2	linear range [ppb]
n-propanal	123-38-6	57.0370	0.9	7.9	0.9996	2.5−118
2-propenal, 2-methyl-	78-85-3	69.0377	0.8	6.6	0.9946	2.4−97
2-pentene, 2-methyl-	625-27-4	84.1004	0.12	5.0	0.9964	0.4−114
acetone	67-64-1	88.0458	1.0	10	0.9997	3−320
n-hexanal	66-25-1	99.0876	0.7	9.0	0.9985	2.1−75
3-buten-2-one	78-94-4	100.0461	1.0	11	0.9984	3−120
2-butanone	78-93-3	102.0616	1.1	7.4	0.9927	4−94
n-heptanal	111-71-7	113.1012	0.35	5.1	0.9980	1−111
5-hepten-2-one, 6-methyl-	110-93-0	126.1134	1.2	10	0.9918	3.5−106
n-octanal	124-13-0	127.1204	0.28	5.9	0.9962	1−86
DL-limonene	5989-27-5	136.1357	0.49	8.2	0.9960	1.5−104
n-nonanal	124-19-6	141.1373	0.36	5.0	0.9944	1−84

[a]Compounds are ordered with respect to the increasing quantifier ions.

lasted 105 min. The time resolution of the measurements amounted to 30 s. This was a trade-off between the method sensitivity and the requirement of the real-time analysis. The temperature and humidity of the air in the chamber were continuously monitored using a B+B TH 309 hygrometer (B +B Thermo-Technik GmbH, Germany).

SRI-TOF-MS Analysis. VOCs were monitored using an Ionicon Analytik (Innsbruck, Austria) type 8000 selective reagent ionization time-of-flight mass spectrometer operating with NO[+] as the reagent ion.[19] The NO[+] ions were produced by supplying the hollow cathode with high purity dry air. The ionization mechanism leading to the formation of NO[+] ions is extensively described elsewhere.[20,21] The settings of the ion source were chosen as follows: ion source current 5 mA, source voltage (U_s) 20 V, source out voltage (U_{so}) 70 V, and source valve 40%. With these settings the parasitic ions H_3O^+, O_2^+, and NO_2^+ were reduced down to the ratio (parasitic ion/NO[+]) of 0.3−0.6%, 1−1.5%, and 1−2%, respectively. The ionization of the analytes contained in the sample gas fed-in at ≈10 mL/min occurred in the drift tube at 2.23 mbar and 60 °C by means of the NO[+] reagent ions extracted from the ion source. Moreover, the drift voltage was set to 600 V leading to an E/N ratio of approximately 130 Td.

The mass spectra ranging from approximately *m/z* 2.76 to *m/z* 500 were acquired at a period of 30 s by coadding 750 000 single TOF-MS extractions of 40 μs duration recorded at the sampling frequency $1/\Delta t$ = 10 GHz. The effective mass resolution obtained from the detected peaks was ≈4000 at *m/z* 100. The mass calibration was based on three peaks always present in the spectra: H_3O^+ (19.0178), [15]NO[+] (30.9945), and NO_2^+ (45.9924).

RESULTS AND DISCUSSION

Ion Chemistry. The reactions of NO[+] (IP, 9.26 eV) with volatile organic compounds are diverse and include charge transfer, hydride ion (H^{−}) transfer, hydroxide ion (OH^{−}) transfer, alkoxide ion (OR[−]) transfer, and NO[+] ion−molecule association.[15,20] Interestingly, different chemical classes of VOCs have their typical reactions with NO[+]. For example, aldehydes react with NO[+] via hydride ion transfer, ketones mainly via ion−molecule association, and aromatic hydro-

carbons via charge transfer.[20] Unfortunately, in the PTR-MS instrument the parent ions frequently fragment during collision with buffer gas molecules producing unspecific secondary ions.[22] Moreover, the data on the fragmentation of volatile organic compounds in SRI-MS are relatively sparse.[22] Consequently, one of the goals of this study was to determine the product ion distribution of the analytes of interest reacting with NO[+].

Table 1 summarizes the product ion distributions of species under study in SRI-TOF-MS working in NO[+] mode. Only the ions with abundance greater than 0.5% of the total product ions signal were considered. In accordance with earlier investigations, aldehydes reacted with NO[+] via hydride ion transfer forming M−H^{+} parent ions.[23] All species from this chemical family fragmented producing 2−6 additional hydrocarbon ions. The most abundant products were formed at the *m/z* 71.0856 ($C_5H_{11}^+$), 57.0699 ($C_4H_9^+$), 43.0562 ($C_3H_7^+$), or 41.0386 ($C_3H_5^+$). Since they occur commonly in the spectra of numerous species (not only aldehydes) they could not be used for the identification and/or quantification of aldehydes under study. Interestingly, heavier *n*-alkanals fragmented less than lighter members of this chemical family. Consequently, the sensitivity for *n*-alkanals in SRI-TOF-MS (NO[+]) increases with the increase of their molecular mass.

Acetone, 2-butanone, and 3-buten-2-one reacting with NO[+] via ion−molecule association[23] exhibited less fragmentation than the aldehydes being their functional isomers. For these compounds the fraction of the NO[+]M ion was greater than 60%. Conversely, the ion−molecule association was not the basic ionization mechanism in the case of 6-methyl-5-hepten-2-one. The NO[+]M channel was very weak (<0.5%) and additionally evidenced the assumptions that the ionization energy (IE) of this compound is lower than the one of NO[+].[24] Instead, 6-methyl-5-hepten-2-one was ionized via charge transfer. The resulting $C_8H_{14}O^+$ ion was further stabilized by ejection of H_2O and CH_3 (or C_2H_2) molecule. The other compounds 2-methyl-2-pentene and DL-limonene reacted with NO[+] via charge transfer; however, they exhibited considerable fragmentation.

The presence of water molecules in the sample had little or no effect on the fragmentation of the molecular ions. However,
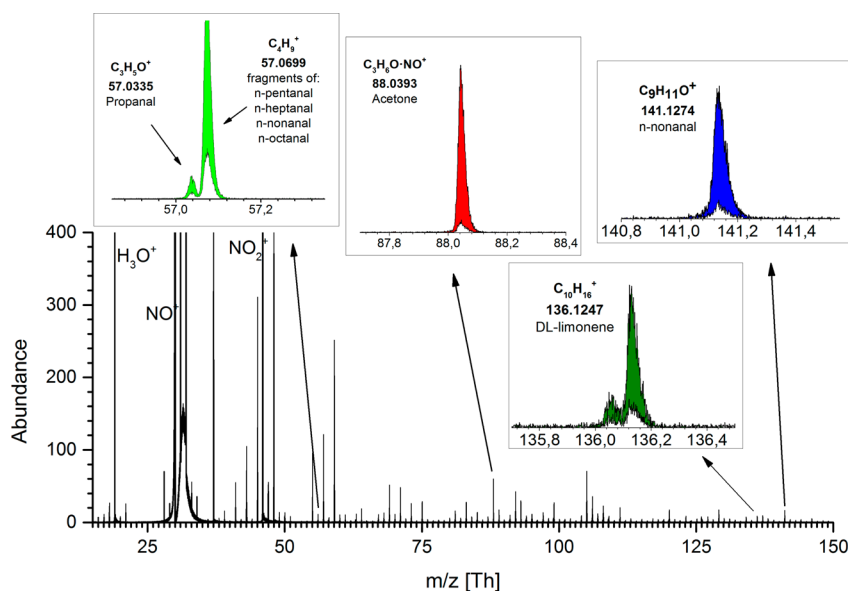
Figure 2. Exemplary SRI-TOF-MS (NO⁺) spectrum from the skin emanation analysis.

several product ions MH⁺ having proton affinities (PA) lower than the one of water (691 kJ mol⁻¹) reacted rapidly with water molecules present in humid samples and thus were eliminated from the reactor. In particular this concerned protonated acetylene $C_2H_3^+$ (PA = 641.4 kJ mol⁻¹) and protonated ethylene $C_2H_5^+$ (PA = 680.5 kJ mol⁻¹) appearing in the *n*-propanal product ion distribution. Moreover, the abundance of the $C_3H_5^+$ product ion was slightly reduced in the spectra of 2-methyl 2-pentene, *n*-hexanal, and *n*-heptanal obtained for humid air. Although the difference between PAs of all possible structural isomers (allene, 775 kJ mol⁻¹; propyne, 748 kJ mol⁻¹; and cyclopropene, 818.5 kJ mol⁻¹) and the one of water should inhibit the proton transfer reaction, it could be promoted by the elevated energies of the ion−molecule interactions in the SRI-TOF-MS and the large number of the H_2O molecules in the humid sample.

Validation Parameters. The calibration curves and validation parameters were determined on the basis of analyses of one-component standard mixtures using the parent (molecular) ions, as indicated in Table 1. The validation parameters for species under study are presented in Table 2.

Limits of detection (LODs) were calculated using the repeated analyses of the blank and the calculation algorithm presented by Huber.[25] More specifically, the standard deviation of 10 consecutive blank (obtained for the zero-air analysis) signals and 1% probability $(1 - \alpha)$ for the type 1 error resulting in the coverage factor of 2.96 were used for these purposes. The LODs ranged from 0.12 ppb for 2-methyl 2-pentene to 1.2 ppb for 6-methyl-5-hepten-2-one (for a measurement time of 30 s). The limit of quantification (LOQ) was defined as 3 × LOD. Relative standard deviations (RSDs) were calculated on the basis of consecutive analyses of five standard mixtures exhibiting concentrations spread around 10 ppb. The RSDs fall within the range of 5.0−11% and were recognized as satisfactory for the goals of this study. The instrument response was found to be linear within the investigated concentration ranges, with coefficients of variation ranging from 0.9918 to 0.9997.

Monitoring of Selected Skin-Borne Volatiles. Within this study emission of 12 skin-borne volatiles were monitored using SRI-TOF-MS (NO⁺). Among them there were six aldehydes (*n*-propanal, *n*-hexanal, *n*-heptanal, *n*-octanal, *n*-nonanal, and 2 methyl 2-propenal), four ketones (acetone, 2-butanone, 3-buten-2-one, and 6-methyl-5-hepten-2-one), one hydrocarbon (2-methyl 2-pentene), and one terpene (DL-limonene). These species were preselected from the set of omnipresent human scent constituents identified and determined in our recent study.[8] Some compounds reported in this reference could not be profiled due to the limitations of the applied technique. This concerned species which could not be satisfactorily separated or produced a weak signal. For example, the separation problem concerned acetaldehyde and the acetone fragment at $C_2H_3O^+$ or isomeric aldehydes (e.g., *n*-pentanal, 2-methyl-butanal, and 3-methyl-butanal). An exemplary SRI-TOF-MS (NO⁺) spectrum from the skin emanation analysis is presented in Figure 2. The initial chamber air temperature was 23.4 ± 1 °C and tended to increase during the volunteer's stay in the chamber by 0.3−3.4 °C (mean 1.9 °C). The relative humidity changed from the ambient values (30−40%) to 70−90%.

Exemplary concentration profiles of acetone, *n*-propanal, *n*-nonanal, *n*-octanal, DL-limonene, and 6-methyl-5-hepten-2-one obtained for the applied protocol are presented in Figure 3. For the majority of species, the background levels were below 2 ppb. Only acetone and *n*-propanal exhibited higher concentrations at the onset of the experiments spreading around the median value of 21 and 4 ppb, respectively. This background did not distort the VOCs concentration profiles and was recognized as satisfactory for the goals of the study. Once the volunteer was closed in the chamber, the skin-borne VOCs accumulated, which was manifested by the increase of their concentration in the chamber air. At the end of this phase, the median absolute concentrations of species under study ranged from 3.5 ppb for DL-limonene to 90 ppb for acetone. The duration of the experiment turned out to be too short to determine unambiguously the characteristic of the VOCs liberation. It seems plausible that the release of some VOCs stemming from the oxidative stress occurring on the skin surface (e.g., aldehydes[12,13,26]) should be reduced shortly after the isolation of the volunteer from the predominant factors
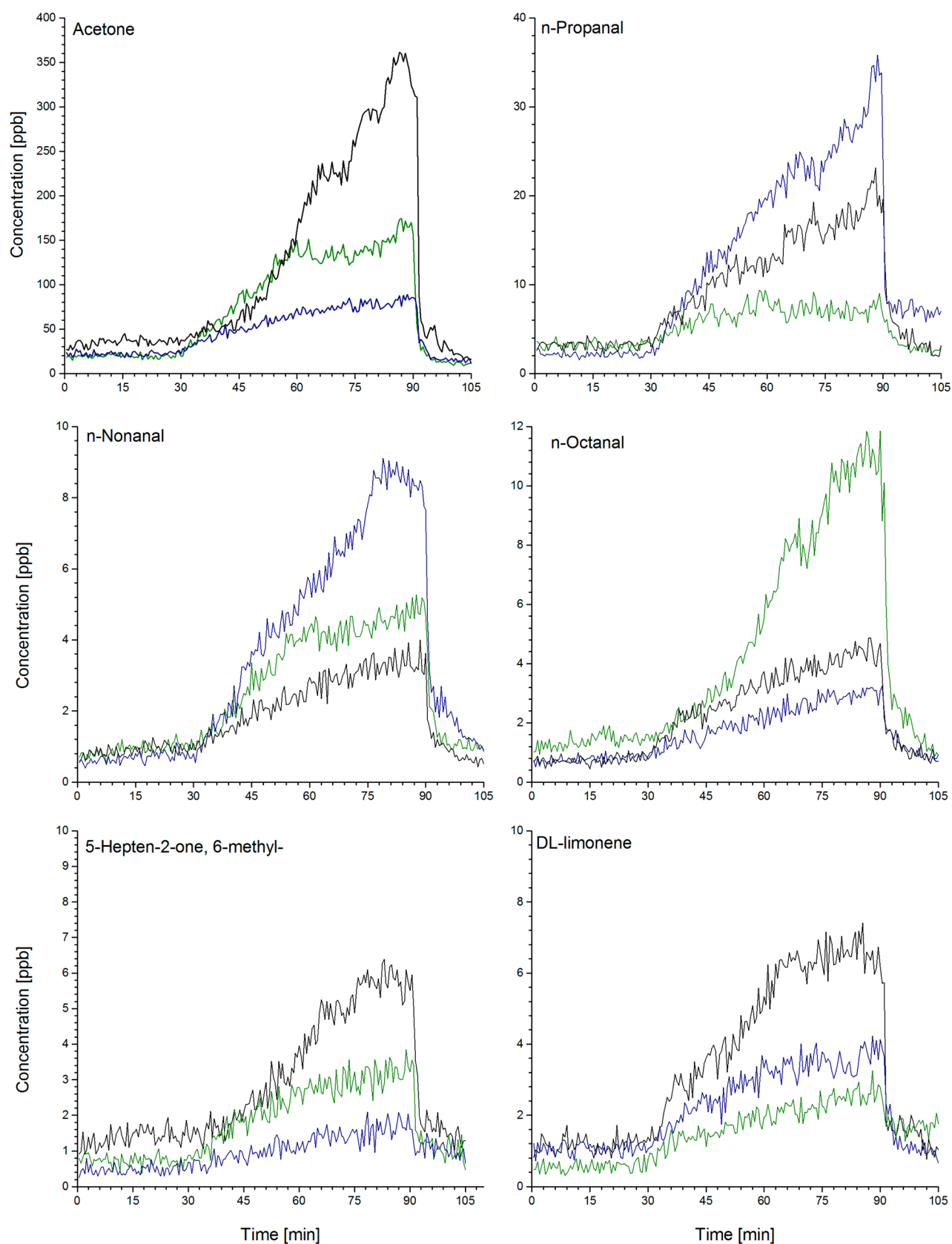
Figure 3. Exemplary concentration profiles of acetone, *n*-propanal, *n*-nonanal, *n*-octanal, DL-limonene, and 6-methyl-5-hepten-2-one. Different colors correspond to three different volunteers.

inducing this condition (O$_3$, UV). Here, the concentrations tended to increase during the whole second phase of the

experiment and the saturation of the concentrations was not observed. Presumably this effect could be noted for the longer

Table 3. Emission Rates and Tentative Origin of Compounds under Study

compound	CAS	emission rate (median) [nmol × min^{-1} × person^{-1}]	emission rate (median) [fmol × min^{-1} × cm^{-2}]	emission rate for arm[8] [fmol × min^{-1} × cm^{-2}]	tentative origin
n-propanal	123-38-6	1.23−19 (4.03)	57−1065 (199)	3.44−112 (12.4)	(a) oxidative degradation of linolenic acid and oleic acid[26]
2-propenal, 2-methyl-	78-85-3	0.22−0.98 (0.55)	10−48 (29)	6.42−55.9 (17.4)	(a) OH-initiated degradation of isoprene[32]
2-pentene, 2-methyl-	625-27-4	0.15−0.55 (0.28)	6.71−28.2 (15.7)	1.05−54 (9.34)	(a) peroxidation of squalene[33]
acetone	67-64-1	13.2−168 (44.8)	792−8010 (1530)	493−3680 (1100)	(a) endogenous decarboxylation of Acetyl-CoA[30] (b) oxidative degradation of squalene[12,13,31]
n-hexanal	66-25-1	1.06−6.33 (1.98)	51.5−301 (105)	16.8−168 (41.9)	(a) oxidative degradation of linoleic acid, palmitoleic acid and vaccenic acid[12,26]
3-buten-2-one	78-94-4	1.57−6.8 (5.76)	73−880 (346)	4.12−19.5 (8.31)	(a) OH-initiated degradation of isoprene[32]
2-butanone	78-93-3	2.4−7.76 (3.94)	122−406 (204)	3.7−16.6 (6.4)	
n-heptanal	111-71-7	0.95−3.27 (1.68)	44−194 (85)	16.8−168 (41.9)	(a) oxidative degradation of linoleic acid, palmitoleic acid and vaccenic acid[34]
5-hepten-2-one, 6-methyl-	110-93-0	0.43−2.54 (0.66)	24−120 (36.3)	14−918 (133)	(a) oxidative degradation of squalene[31,12,13]
n-octanal	124-13-0	0.5−2.52 (0.99)	30−143 (52)	22.5−150 (33.1)	(a) oxidative degradation of oleic acid[12,13,26]
DL-limonene	5989-27-5	0.21−2.39 (0.76)	11−113 (37.5)	0.88−377 (8.76)	(a) diet (flavoring)[35] (b) cosmetics, solvents
n-nonanal	124-19-6	0.58−5.22 (1.52)	35−248 (79)	18.1−119 (58.9)	(a) oxidative degradation of oleic acid[12,13,26]

subjects' presence in the chamber. Unfortunately, the prolongation of the experiment time was recognized as oppressive by the majority of the volunteers and could not be applied. Consequently, for the investigated time period constant VOCs emissions were assumed. For such an assumption the VOC emission rate is expressed by the slope of the concentration profile recorded during the experiment phase involving a human subject. The slopes, which were computed by fitting the linear function to the corresponding concentration data together with the volunteers' characteristics and experiment conditions, were used to calculate emission rates of analytes of interest. These were expressed in nanomoles of analyte emitted by the person within 1 min of the experiment (nmol person^{-1} min^{-1}) and alternatively in femtomoles released by one square centimeter of skin within 1 min (fmol cm^{-2} min^{-1}). In case of the latter, the volunteer's skin area was estimated using the formula given by Mosteller.[27] The computed values are given in Table 3.

The presence of aldehydes in human odor is related to the oxidation of human sebum.[12,28] This unique continuous layer of lipids has photoprotective, antibacterial, and antimycotic properties and is believed to be a natural antioxidant capable of neutralizing reactive oxygen species (ROS).[1,29] While exposed to ROSs, sebum constituents degrade releasing a wide range of volatiles including aldehydes. More specifically, aldehydes are produced from skin fatty acids via β-scission of alkoxy radicals formed by the homolytic cleavage of hydroperoxides.[26] For example, n-octanal was reported to stem from oleic acid,[13,26] whereas, n-hexanal was demonstrated to be formed from linoleic, palmitoleic, and vaccenic acids.[13,26] The median emission rates of the investigated aldehydes ranged from 29 fmol cm^{-2} min^{-1} for 2 methyl 2-propenal to 199 fmol cm^{-2} min^{-1} for n-propanal. These values are in a good agreement with the emission rates noted for the forearm skin in our recent study (see Table 3). Since the human sebum is thicker on the skin covering central parts of the body (e.g.,

chest or forehead[9]) it is not surprising that the emission rates recorded within this study reflect this uneven distribution and are somewhat elevated. With the exception of n-propanal, these differences amounted to 40−150%. Much more pronounced discrepancy was observed for n-propanal. This may result from the low number of volunteers affecting the statistics, superposition of signals from other species at the m/z 57.0335, or both.

Four ketones were monitored within this study: acetone, 2-butanone, 3-buten-2-one, and 6-methyl-5-hepten-2-one. The emission rate of acetone was spread around the median value of 1530 fmol cm^{-2} min^{-1} and was at least 1 order of magnitude higher than the emission rates of the remaining species. This is not surprising as at least two productive sources of this compound can be indicated. First, acetone is produced in large amounts endogenously in the liver during spontaneous decarboxylation of acetoacetate.[30] Second, it is formed on human skin during induction by reactive oxygen species degradation of squalene.[12,13,31] Since squalene is the major component of human sebum it seems plausible that the acetone emission reflects this high abundance. The whole skin emission of acetone was approximately 50% higher than the emission from forearm skin (see Table 3) mirroring presumably the aforementioned sebum distribution. Interestingly, the analogous differences for 2-butanone and 3-buten-2-one were considerably higher. Apart from ketones, only several classes of VOCs react with NO$^+$ via ion−molecule association. These include esters, carboxylic acids, and some hydrocarbons.[20] However, the exact mass measurement of the respective molecular ions excludes members of these chemical classes as potential sources of the signal distortion. Conversely, the emission rate of 6-methyl-5-hepten-2-one was 3-fold lower when measured for the whole skin than for the limb skin. The reason of this discrepancy remains unclear.

CONCLUSIONS

The present study aimed at the monitoring of whole-skin emission of selected potential markers of entrapped humans. For this purpose selective reagent ionization time-of-flight mass spectrometry operating in NO^+ mode and a bodyplethysmography chamber mimicking the entrapment scene were applied. Overall profiles of 12 volatiles were quantitatively monitored in skin emanation of 10 volunteers over a time period of 1 h. The observed median emission rates ranged from 0.28 to 44.8 nmol person^{-1} min^{-1} for 2-methyl-2-pentene and acetone, respectively (or 16−1530 fmol cm^{-2} min^{-1}) and were higher than the emission rated observed for peripheral (forearm) skin.

The findings of this study provide quantitative information about the formation of the human chemical fingerprint, which could be used for early location of entrapped victims during USaR operations. The understanding of the production and initial composition of this signature is of particular importance for modeling of its behavior in the surroundings of the entrapped person. Moreover, the concentration levels and physicochemical characteristics of the potential markers of human presence determine the selection of analytical instruments, which could be used for the field detection of entombed victims. Such an on-site, real-time, and hand-held instrumentation could considerably improve the effectiveness of USaR operations. A number of recent studies suggest that some analytical techniques such as ion mobility spectrometry (multicapillary column-ion mobility spectrometry (MCC-IMS), aspiration ion mobility spectrometry (AIMS), field asymmetric waveform ion mobility spectrometry (FAIMS)) or sensor boards could meet this requirement and open a new promising window in the USaR field operations toward the fast detection of entrapped humans.

AUTHOR INFORMATION

Corresponding Authors

*E-mail: pawel.mochalski@uibk.ac.at. Phone: +43-512-504-24636. Fax: +43-512-504-6724636.
*E-mail: anton.amann@i-med.ac.at.

Notes

The authors declare no competing financial interest.

ACKNOWLEDGMENTS

REFERENCES

(1) de Lacy Costello, B.; Amann, A.; Al-Kateb, H.; Flynn, C.; Filipiak, W.; Ratcliffe, N. M. *J. Breath Res.* **2014**, *8*, No. 014001.

(2) Filipiak, W.; Ruzsanyi, V.; Mochalski, P.; Filipiak, A.; Bajtarevic, A.; Ager, C.; Denz, H.; Hilbe, W.; Jamnig, H.; Hackl, M.; Dzien, A.; Amann, A. *J. Breath Res.* **2012**, *6*, No. 036008.

(3) Amann, A., Smith, D., Eds. *Volatile Biomarkers: Non-Invasive Diagnosis in Physiology and Medicine*; Elsevier: Amsterdam, The Netherlands, 2013.

(4) Huo, R.; Agapiou, A.; Bocos-Bintintan, V.; Brown, L. J.; Burns, C.; Creaser, C. S.; Devenport, N. A.; Gao-Lau, B.; Guallar-Hoyas, C.; Hildebrand, L.; Malkar, A.; Martin, H. J.; Moll, V. H.; Patel, P.; Ratiu, A.; Reynolds, J. C.; Sielemann, S.; Slodzynski, R.; Statheropoulos, M.; Turner, M. A.; Vautz, W.; Wright, V. E.; Thomas, C. L. *J. Breath Res.* **2011**, *5*, No. 046006. Vautz, W.; Slodzynski, R.; Hariharan, C.; Seifert, L.; Nolte, J.; Fobbe, R.; Sielemann, S.; Lao, B. C.; Huo, R.; Thomas, C. L.; Hildebrand, L. *Anal. Chem.* **2013**, *85*, 2135−2142. Mochalski, P.; Krapf, K.; Ager, C.; Wiesenhofer, H.; Agapiou, A.; Statheropoulos, M.; Fuchs, D.; Ellmerer, E.; Buszewski, B.; Amann, A. *Toxicol. Mech. Methods* **2012**, *22*, 502−511. Agapiou, A.; Mochalski, P.; Schmid, A.; Amann, A. In *Volatile Biomarkers: Non-invasive Diagnosis in Physiology and Medicine*; Amann, A., Smith, D., Eds.; Elsevier: Amsterdam, The Netherlands, 2013, pp 515 − 558.

(5) Ferworn, A. In *Canine Ergonomics: The Science of Working Dogs*, Helton, W. S., Ed.; CRC Press: Boca Raton, FL, 2009; pp 205−244.

(6) Wong, J.; Robinson, C. *Urban Search and Rescue Technology Needs: Identification of Needs*; Federal Emergency Management Agency (FEMA) and the National Institute of Justice (NIJ), Document number 207771.2004.

(7) Bartels, S. A.; Vanrooyen, M. J. *Lancet* **2012**, *379*, 748−757.

(8) Mochalski, P.; King, J.; Unterkofler, K.; Hinterhuber, H.; Amann, A. *J. Chromatogr., B* **2014**, submitted.

(9) De Luca, C.; Valacchi, G. *Mediat. Inflamm.* **2010**, *2010*, No. 321494.

(10) Lindinger, W.; Hansel, A.; Jordan, A. *Int. J. Mass Spectrom. Ion Processes* **1998**, *173*, 191−241. Hansel, A.; Jordan, A.; Holzinger, R.; Prazeller, P.; Vogel, W.; Lindinger, W. *Int. J. Mass Spectrom. Ion Processes* **1995**, *149/150*, 609−619.

(11) King, J.; Kupferthaler, A.; Frauscher, B.; Hackner, H.; Unterkofler, K.; Teschl, G.; Hinterhuber, H.; Amann, A.; Hogl, B. *Physiol. Meas.* **2012**, *33*, 413−428. King, J.; Unterkofler, K.; Teschl, G.; Teschl, S.; Koc, H.; Hinterhuber, H.; Amann, A. *J. Math. Biol.* **2011**, *63*, 959−999. Muller, K.; Haferkorn, S.; Grabmer, W.; Wisthaler, A.; Hansel, A.; Kreuzwieser, J.; Cojocariu, C.; Rennenberg, H.; Herrmann, H. *Atmos. Environ.* **2006**, *40*, S81−S91.

(12) Wisthaler, A.; Weschler, C. J. *Proc. Natl. Acad. Sci. U.S.A.* **2010**, *107*, 6568−6575.

(13) Wisthaler, A.; Tamas, G.; Wyon, D. P.; Strom-Tejsen, P.; Space, D.; Beauchamp, J.; Hansel, A.; Mark, T. D.; Weschler, C. J. *Environ. Sci. Technol.* **2005**, *39*, 4823−4832.

(14) Kohl, I.; Beauchamp, J.; Cakar-Beck, F.; Herbig, J.; Dunkl, J.; Tietje, O.; Tiefenthaler, M.; Boesmueller, C.; Wisthaler, A.; Breitenlechner, M.; Langebner, S.; Zabernigg, A.; Reinstaller, F.; Winkler, K.; Gutmann, R.; Hansel, A. *J. Breath Res.* **2013**, *7*, 017110.

(15) Jordan, A.; Heidacher, S.; Hanel, G.; Hartungen, E.; Herbig, J.; Maerk, L.; Schottkowsky, R.; Seehauser, H.; Siulzer, P.; Maerk, T. D. *Int. J. Mass Spectrom.* **2009**, *286*, 32−38.

(16) Sulzer, P.; Edtbauer, A.; Hartungen, E.; Jurshcik, S.; Jordan, A.; Hanel, G.; Feil, S.; Jaksch, S.; Mark, L.; Mark, T. D. *Int. J. Mass Spectrom.* **2012**, *321−322*, 66−70.

(17) Gallagher, M.; Wysocki, C. J.; Leyden, J. J.; Spielman, A. I.; Sun, X.; Preti, G. *Br. J. Dermatol.* **2008**, *159*, 780−791. Curran, A. M.; Prada, P. A.; Furton, K. G. *J. Forensic Sci.* **2010**, *55*, 50−57.

(18) Mochalski, P.; King, J.; Klieber, M.; Unterkofler, K.; Hinterhuber, H.; Baumann, M.; Amann, A. *Analyst* **2013**, *138*, 2134−2145.

(19) Karl, T.; Hansel, A.; Cappellin, L.; Kaser, L.; Herdlinger-Blatt, I.; Jud, W. *Atmos. Chem. Phys.* **2012**, *12*, 11877−11884.

(20) Smith, D.; Spanel, P. *Mass Spectrom. Rev.* **2005**, *24*, 661−700.

(21) Federer, W.; Dobler, W.; Howorka, F.; Lindinger, W.; Durupferguson, M.; Ferguson, E. E. *J. Chem. Phys.* **1985**, *83*, 2032−2038.

3922

dx.doi.org/10.1021/ac404242q | *Anal. Chem.* 2014, 86, 3915−3923

(22) Schwarz, K.; Filipiak, W.; Amann, A. *J. Breath Res.* **2009**, *3*, No. 027002. Buhr, K.; van Ruth, S.; Delahunty, C. *Int. J. Mass Spectrom.* **2002**, *221*, 1−7.

(23) Spanel, P.; Ji, Y.; Smith, D. *Int. J. Mass Spectrom. Ion Processes* **1997**, *165*, 25−37.

(24) Amelynck, C.; Schoon, N.; Kuppens, T.; Bultinck, P.; Arijs, E. *Int. J. Mass Spectrom.* **2005**, *247*, 1−9.

(25) Huber, W. *Accred. Qual. Assur.* **2003**, *8*, 213−217.

(26) Frankel, E. N. *Prog. Lipid Res.* **1980**, *19*, 1−22. Fujisaki, M.; Endo, Y.; Fujimoto, K. *J. Am. Oil Chem. Soc.* **2002**, *79*, 909−914.

(27) Mosteller, R. D. *N. Engl. J. Med.* **1987**, *317*, 1098.

(28) Lee, S. H.; Jeong, S. K.; Ahn, S. K. *Yonsei Med. J.* **2006**, *47*, 293−306. Pappas, A.; Anthonavage, M.; Gordon, J. S. *J. Invest. Dermatol.* **2002**, *118*, 164−171. Thiele, J. J.; Weber, S. U.; Packer, L. *J. Invest. Dermatol.* **1999**, *113*, 1006−1010.

(29) Ryu, A.; Arakane, K.; Koide, C.; Arai, H.; Nagano, T. *Biol. Pharm. Bull.* **2009**, *32*, 1504−1509.

(30) Schwarz, K.; Pizzini, A.; Arendacka, B.; Zerlauth, K.; Filipiak, W.; Schmid, A.; Dzien, A.; Neuner, S.; Lechleitner, M.; Scholl-Burgi, S.; Miekisch, W.; Schubert, J.; Unterkofler, K.; Witkovsky, V.; Gastl, G.; Amann, A. *J. Breath Res.* **2009**, *3*, 027003.

(31) Fruekilde, P.; Hjorth, J.; Jensen, N. R.; Kotzias, D.; Larsen, B. *Atmos. Environ.* **1998**, *32*, 1893−1902.

(32) Dibble, T. S. *J. Phys. Chem. A* **1999**, *103*, 8559−8565.

(33) Stein, R. A.; Mead, J. F. *Chem. Phys. Lipids* **1988**, *46*, 117−120.

(34) Haze, S.; Gozu, Y.; Nakamura, S.; Kohno, Y.; Sawano, K.; Ohta, H.; Yamazaki, K. *J. Invest. Dermatol.* **2001**, *116*, 520−524.

(35) Yannai, S., Ed. *Dictionary of Food Compounds with CD-ROM: Additives, Flavors, and Ingredients*; Chapman & Hall/CRC: Boca Raton, FL, 2004.

3923

dx.doi.org/10.1021/ac404242q | *Anal. Chem.* 2014, 86, 3915−3923